Trypanosome CNOT10 is essential for the integrity of the NOT deadenylase complex and for degradation of many mRNAs

Valentin Färber[1], Esteban Erben[1], Sahil Sharma[2], Georg Stoecklin[2] and Christine Clayton[1],*

[1]DKFZ-ZMBH Alliance, Zentrum für Molekulare Biologie der Universität Heidelberg and [2]DKFZ-ZMBH Alliance, Deutsche Krebsforschungszentrum, Im Neuenheimer Feld 282, D69120 Heidelberg, Germany

ABSTRACT

The degradation of most eukaryotic mRNAs is initiated by removal of the poly(A) tail, and the major deadenylase activity is associated with the CCR4/CAF1/NOT complex (NOT complex). We here study the role of CNOT10, a protein that is found in human and trypanosome, but not in yeast, NOT complexes. Trypanosome (*Tb*) CNOT10 is essential for growth. *Tb*CNOT10 interacted with the deadenylase *Tb*CAF1 and the scaffold protein *Tb*NOT1; *Tb*CAF1 also interacted with *Tb*NOT1 in a yeast two-hybrid assay. In both trypanosomes and human embryonic kidney cells, approximately half of CAF1 was associated with the NOT complex. Depletion of CNOT10 from human cells did not affect this association. In contrast, depletion of *Tb*CNOT10 in trypanosomes caused a decrease in the level of *Tb*NOT1, detachment of *Tb*CAF1 from the complex and pronounced stabilization of most trypanosome mRNAs. Artificial tethering of *Tb*CAF1 to a reporter mRNA *in vivo* resulted in mRNA degradation, and this was not affected by *Tb*CNOT10 depletion. We conclude that in trypanosomes, *Tb*CNOT10 may stabilize the interaction between *Tb*CAF1 and the NOT complex. The results further suggest that *Tb*CAF1 is only able to deadenylate mRNA *in vivo* if it is recruited to the mRNA through other NOT complex components.

INTRODUCTION

The degradation of mRNAs is important for control of gene expression. In eukaryotes, the degradation of most mRNAs is initiated by removal of the poly(A) tail. Decay then proceeds either from the 3′ end, by the exosome, or from the 5′ end by decapping and subsequent digestion by the exoribonuclease XRN1 (1). Three cytosolic deadenylases have been described in eukaryotes: the poly(A) ribonucleases; the poly(A) nuclease Pan2 with its co-factor Pan3; and CCR4 and CAF1, both of which are part of the CCR4–CAF1–NOT complex (hereafter simply called 'the NOT complex') (2). The NOT complex has been found to be the most important effector of mRNA deadenylation (3–5). In addition, it has been implicated in the regulation of transcription, the DNA damage response, nuclear surveillance, mRNA export and translation repression (6).

In all eukaryotes examined so far, the NOT complex consists of at least seven subunits. In yeast, the universally conserved subunits are called Caf1p, Caf40p and Not1p, Not2p and Not5p (5,7–11). Not1p (human CNOT1, *Drosophila* and trypanosome NOT1) acts as a platform for the remaining core subunits. In human cells, it is also recruited by GW182/TNRC6 for miRNA-induced mRNA decay (12) and by Tis11 proteins, which mediate degradation of mRNAs with AU-rich elements (6,13). The central role of NOT1 as a scaffold is shown by the fact that in human cells and yeast, its depletion disrupts the complex and abrogates mRNA deadenylation (14,15). The major deadenylase activity in the human, *Trypanosoma* and *Drosophila* complexes is CAF1; there are two paralogues in humans, called Caf1a/b or CNOT7 and CNOT8. Animal cells and yeast have an additional deadenylase called CCR4 or Ccr4p; in yeast, Ccr4p is more active than Caf1p (4–6). Recent crystal structures for relevant fragments of the yeast and human Not1 and Caf1 proteins have shown that they are held together mainly through hydrophobic interactions (16,17).

The functions of the remaining core subunits are not clear. Yeast has two proteins equivalent to NOT5: Not3p and Not5p. Although these are 44% identical, the corresponding mutant strains showed specific gene expression changes, suggesting that the two subunits have distinct roles (15). NOT2 (human CNOT2) is important for complex integrity, as it seems to link NOT3/5 to NOT1

(15,18,19). The role of Caf40p (human Rcd-1) is unknown, although Rcd-1 can dimerize and bind single-stranded DNA (20). In yeast, Not4p is associated with the NOT complex (21); it is an E3 ligase involved in degrading aberrant polypeptides that lack a stop codon (22) and may act independently of the other subunits. The homologues in human cells (CNOT4) and *Drosophila* are not stably associated with the complex (9,10) and there is no homologue in trypanosomes (5).

The remaining subunits are less widely distributed in evolution. Caf130p, which is found exclusively in fungi, interacts with the N- and C-termini of Not1p, but is not important for the stability of the complex (15,23). Two more subunits have been identified in human cells: TAB182 and C2ORF29 (9). This article concentrates mainly on CNOT10, which has been described in human cells but is absent from fungi. Tandem affinity purification (TAP) of human CNOT10 retrieved all core subunits of the complex, but not the deadenylases (9); apart from that nothing is known about CNOT10 function.

The parasite *Trypanosoma brucei*, and related kinetoplastid protists, have an exceptional genome organization. Protein-coding genes are arranged in large polycistronic units transcribed by RNA polymerase II (24). Cleavage and maturation of the precursor mRNA are initiated by *trans*-splicing, which places identical leader sequences at the 5′-end of every mRNA; this is coupled to polyadenylation of the mRNA immediately upstream (25,26). As a consequence of this gene arrangement, the parasite lacks transcriptional control of individual protein-coding genes. Transcript levels are determined mainly by gene copy number and mRNA degradation rates (27). We have previously shown that the degradation of most trypanosome mRNAs is initiated by deadenylation (27). TAP of *T. brucei* CAF1 identified all core subunits of the complex, including a distant relative of *Homo sapiens* (*Hs*) CNOT10 (5). In this report, we analyse the role of *Tb*CNOT10 in *trypanosomes* and compare some results with those seen for its counterpart in human cells.

MATERIALS AND METHODS

Cell culture

The experiments were done with bloodstream-form *T. brucei* that stably express the tetracycline repressor, with or without T7 polymerase expression. Culturing, transfections and RNAi experiments were conducted as described earlier (28). mRNA decay was analysed after 24 h of RNAi targeting *TbCNOT10*. Cells were treated with Sinefungin (final concentration 2 μg/ml) for 5 min, and then actinomycin D was added to a final concentration of 10 μg/ml.

Human embryonic kidney (HEK) 293 cells were cultured in Dulbecco's-modified Eagle medium (DMEM) containing 10% fetal bovine serum (PAA Laboratories), 2 mM L-glutamine, 100 U/ml penicillin and 0.1 mg/ml streptomycin (all PAN Biotech) at 37°C/5% CO_2. Cells were transfected with DNA using polyethyleneimine (PEI) (Polysciences Europe; 1 mg/ml, pH 7.0) at a ratio of 1:2 (DNA:PEI) in serum-free DMEM without antibiotics. For transfection of siRNAs, Lipofectamine RNAimax (Invitrogen) and Optimem (Gibco) were used according to the manufacturer's protocol. siRNAs were transfected at a concentration of 100 nM with Lipofectamine RNAimax twice over a time period of 4 days. Medium was changed to regular DMEM 4 h after transfection of DNA.

Lists of plasmids, primers and siRNAs used in this article are in Supplementary Table S1.

RNA extraction and northern blot analysis

Total RNA was extracted using peqGold Trifast (peqLab, Germany). RNA was run on 1.5% formaldehyde gels or 4.5% polyacrylamide-urea gels and blotted onto Nytran membranes (GE Healthcare). RNase H digestion with oligo d(T) was adapted from the method described previously (5). Ten micrograms of RNA was mixed with 170 pmol oligo d(T) and RNAse H buffer (New England Biolabs) and filled up with water to 50 μl. The mixture was denatured at 85°C for 5 min, incubated at 42°C for 10 min, then further cooled over 15 min at 32°C. One microlitre of RNasin® RNase Inhibitor (Promega) and 5 U RNaseH (New England Biolabs) were added and the reaction incubated at 37°C for 1 h.

Northern blots were hybridized with radioactively labelled DNA (Prime-IT RmT Random Primer Labelling Kit, Stratagene) or RNA (MAXIscript, Ambion) probes. Signals were measured using a phosphorimager. For trypanosome RNA, either the signal of the signal recognition particle (*7SL*) or a large subunit rRNA (*LSU1*) was used for normalization. The half-lives were estimated using only those segments of the time course that gave exponential decay curves (fitted with a linear correlation coefficient generally exceeding 0.9).

Co-immunoprecipitation

To make trypanosome extracts, 5×10^7 trypanosomes were re-suspended in immunoprecipitation (IP) lysis buffer (10 mM NaCl, 10 mM Tris–HCl, pH 7.5, 0.3% IGEPAL and protease inhibitors [Protease Inhibitor Mixture {ethylenediaminetetraacetic acid (EDTA)-free}; Roche Applied Science]) and passed five times through a 27-gauge syringe. The resulting extracts were centrifuged for 20 min at 4°C, at $16\,000 \times g$. The supernatant was transferred into a new tube and the salt concentration was adjusted to 180 mM NaCl. To test the RNA dependence of interactions, RNaseA was added to the lysis and wash buffers at a concentration of 200 μg/ml, with or without RNasin® Ribonuclease inhibitor (Promega) at a concentration of 48 μg/ml.

For IP, 30 μl of anti-V5-antibody- or anti-c-myc-antibody-coupled agarose (both from Bethyl Laboratories) was washed four times with 1× phosphate buffered saline (PBS) and once with IP lysis buffer adjusted to 180 mM NaCl at 4°C, with centrifugation at $0.9 \times g$ for 2 min. A sample equivalent to 5×10^5 cells was taken from the input lysate and 2× Laemmli buffer was added. The remainder of the lysate was then added to the beads, and the mixture incubated for 1–1.5 h at 4°C with

rotation. After centrifugation, the supernatant was transferred to another tube and a sample equivalent to 5×10^5 cells was again taken and $2\times$ Laemmli buffer was added. The remaining beads were washed four times for 5 min at 4°C with salt-adjusted lysis buffer, with intermediate centrifugation, then boiled in $2\times$ Laemmli buffer.

For human cells, 24 h after transient transfection, HEK293 cells from a confluent 10 cm dish were collected and lysed in 400 µl ice-cold RNA-IP lysis buffer (50 mM Tris [pH 8.0], 150 mM NaCl, 1 mM $MgCl_2$, 2% NP-40 and 10% glycerol with freshly added protease inhibitors [Complete; Roche]). Nuclei were removed by centrifugation at $500 \times g$ for 5 min at 4°C. A total of 30 µl of streptavidin sepharose beads (GE Healthcare) was added for an additional 1.5–2 h and washed six times in NET2 buffer (50 mM Tris [pH 7.5], 150 mM NaCl and 0.5% Triton X-100). Protein complexes were eluted with 50 µl sodium dodecyl sulphate (SDS) sample buffer with 100 mM dithiothreitol (DTT). Proteins were resolved on 5–20% gradient polyacrylamide gels and transferred onto a 0.2-µm pore size nitrocellulose membrane (Peqlab) for western blotting. Horseradish peroxidase-coupled secondary antibodies (Jackson Immunoresearch) in combination with Western Lightning-enhanced chemiluminescence substrate (Perkin Elmer) were used for detection. Streptavidin sepharose beads (GE Healthcare) were used to purify myc-Strep-tagged (myc-SG) proteins.

Two-hybrid analysis

Complete trypanosome open reading frames (ORFs) were cloned into pGADT7 (GAL4 activation domain vector) and pGBKT7 (GAL4 DNA-binding domain vector) (Matchmaker 3 System, Clontech). The two-hybrid yeast strain AH109 was then transformed with these plasmids in all possible combinations. The expression of the fusion protein was confirmed by western blot analysis using antibody to the HA epitope of the GAL4 activation domain fusion proteins, and antibody to the c-myc epitope of the GAL4 DNA-binding domain fusions. Transformants were selected on four drop-out (SD/-Trp/-Leu/-His/-Ade) culture plates after 4 days of incubation at 30°C, and the resulting positive clones were assayed for β-galactosidase activity using a colony-lift filter assay. Alternatively, reporter activation was tested by replica plating on triple drop-out plates: SD/-Trp/-Leu/-His (medium stringency). As negative controls for self-activation, we used combinations of the *Tb*NOT-complex subunits with CLONTECH vectors pGAD-T-antigen and pGBKT7-p53. Further, p53 (pGBKT7-p53) and SV40 large T-antigen (pGADT7-T) cotransformants were used as positive controls, whereas lamin C (pGBKT7-Lamin) and pGADT7-T cotransformants were used as negative controls.

Glycerol gradients

Trypanosomes (3×10^7), or HEK293 cells from a confluent 10 cm dish, were washed with $1 \times$ PBS, then frozen in liquid nitrogen and stored at −80°C until use. The cell pellets were thawed on ice and re-suspended in ice-cold buffer containing 10 mM Tris–HCl, pH 7.6, 10 mM NaCl, 10 mM MgCl and protease inhibitors (Protease Inhibitor Mixture [EDTA-free]; Roche Applied Science), then forced five times through a 27-g needle. IGEPAL CA-630 (Sigma) was added to a final concentration of 0.1% and the cells were again forced through the needle five times. The lysate was centrifuged first for 20 min at 4°C, $10\,000 \times g$, then the supernatant was spun for 1 h at $100\,000\times$ at 4°C. The final supernatant was layered onto a 12-ml 10–30% glycerol gradient (200 mM KAc, 20 mM Tris–HCl, pH 8.0, 5 mM MgAc, 1 mM DTT and protease inhibitors [Protease Inhibitor Mixture {EDTA-free}; Roche Applied Science]), which was then spun at $229\,900 \times g$ for 17 h at 4°C. Twenty-seven fractions were taken from the top at 23-s intervals. The fractions were incubated on ice overnight with 15% trichloroacetic acid, 0.1% DOC and 10 µg bovine serum albumin (BSA). Precipitates were washed with acetone and re-suspended in Laemmli buffer.

Tandem affinity purification

Trypanosomes 2.5×10^{10} were harvested and used for TAP as previously described (29). The eluate was run 1 cm into a 10% SDS–polyacrylamide gel electrophoresis (PAGE) resolving gel and stained with colloidal Coomassie. The protein-containing gel area was cut into five slices, which were analysed by mass spectrometry.

Protein detection

Trypanosomes or HEK cells were washed once with PBS then dissolved in $2\times$ Laemmli buffer. Protein samples were run on a SDS–PAGE, then blotted onto an Optitran BA-S 85 reinforced NC 0.45 µm membrane (Whatman, Dassl, Germany). The blots were probed with appropriate antibodies and then developed with Western Lightning®-ECL solution (Perkin Elmer).

Immunofluorescence (IF) microscopy was conducted as described earlier in (5). The following antibodies were used in western blotting: monoclonal mouse Anti-V5 (Santa Cruz), monoclonal mouse anti c-myc (Santa Cruz), monoclonal mouse anti-GFP (Santa Cruz), ECL™ Anti-Rabbit IgG (GE Healthcare), ECL™ Anti-Mouse IgG (GE Healthcare), polyclonal rabbit antibodies anti-myc (A-14, sc-789, Santa Cruz), anti-*Hs*CNOT10 (15938-1-AP, Protein Tech) and anti-*Hs*CNOT1 (14276-1-AP, Protein Tech); polyclonal anti-trypanosome aldolase (30). Polyclonal rabbit anti-Caf1a was kindly provided by Ann-Bin Shyu (University of Texas, Houston, TX, USA) and monoclonal antibody to trypanosome tubulin was from Keith Gull (31).

We expressed recombinant His-tagged *Tb*CNOT10 (full length) in *Escherichia coli* but it was very poorly soluble and we were unable to elute it specifically from the nickel column. A preparation of adequate quality for immunization was not obtained.

Database searches

To find potential homologues of Tb927.10.8720, (old number Tb10.6k15.1820), the protein sequence was analysed by BLASTp, psi-BLAST and tBLAST (32). We

used standard parameters and excluded kinetoplastids (taxid:5653) from the search. Domains were identified by a SUPERFAMILY search (33). To find conserved regions in the protein sequence, multiple sequence alignments were done with ClustalW.

RESULTS

Phylogenetic sequence analysis of *Tb*CNOT10

The protein encoded by trypanosome locus *Tb*927.10.8720 was previously identified as a potential component of the NOT complex through TAP of *Tb*CAF1 (5). It is 555 amino acids long, with tetratricopeptide repeat (TPR)-like domains in positions 199–313 and 471–550. BLASTp and psi-BLAST searches on the whole Genbank database (excluding kinetoplastids) identified, as matches, >40 orthologues of CNOT10 in plants and animals, with *E*-values ranging from 3×10^{-4} to 1×10^{-7}. The regions that matched covered 20–60% of the proteins, with identities of 20–30%. Reciprocal BLASTp of human CNOT10 (*Hs*CNOT10) against the *T. brucei* genome yielded *Tb*927.10.8720 as the best match (*E*-value 3×10^{-4}). Most matches with other CNOT10s were located in the beginning of the first *Tb*CNOT10 TPR domain (Figure 1A). We also did directed BLASTp searches using human or trypanosome CNOT10 to probe different eukaryotic phyla and kingdoms: we were unable to find equivalents to CNOT10 in Apicomplexa, Diplomonadida, Alveolates and fungi, but it is present in plants. We concluded that Tb927.10.8720 might be homologue of human CNOT10, so we provisionally named it *Tb*CNOT10.

*Tb*CNOT10 is a component of the NOT complex

To confirm *Tb*CNOT10 as a member of the NOT complex, we conducted IPs. We used trypanosomes expressing tagged versions. The *Tb*CNOT10 gene was tagged *in situ*, by homologous recombination with a sequence encoding an N-terminal V5-tag. *Tb*CAF1 with a C-terminal myc tag (CAF1-myc) was expressed from a tetracycline-inducible promoter. A pull-down of V5-tagged *Tb*CNOT10 (V5-*Tb*CNOT10) resulted in coprecipitation of *Tb*CAF1-myc (Figure 1B) and vice versa (Supplementary Figure S1). RNaseA treatment did not disrupt the interaction (not shown).

In order to identify further proteins that are stably associated with *Tb*CNOT10, we generated trypanosomes in which a TAP-tag-coding sequence was integrated directly upstream of the *Tb*CNOT10 ORF. In IF microscopy, TAP-tagged *Tb*CNOT10 was detected in a rather granular pattern in the cytoplasm (Figure 1D). After TAP of *Tb*CNOT10, all associated proteins were analysed by mass spectrometry (Supplementary Table S2). We found all previously known members of the trypanosome NOT complex except *Tb*CAF1; they included the uncharacterized Tb927.8.1960 protein, which had been seen in the previously published purification (5). These results confirmed that *Tb*CNOT10 is a stable component of the trypanosome NOT complex. Previous results from human cells were similar: after purification

of the TAP-tagged *Hs*CNOT10, neither *Hs*CNOT6/6L (CCR4) nor *Hs*CNOT7 (CAF1a) was found (9). *Tb*CAF40 (Tb927.4.410), which had not been found in our published purification using TAP-tagged CAF1 (5), was detected in the CNOT10 preparation. We also found *Tb*DHH1 (as seen previously with *Tb*CAF1).

There was also a number of novel potential NOT-associated proteins. These included three ATP-dependent DEAD/H RNA helicases (Tb927.3.2600, Tb927.8.1510 and Tb09.211.3510), two of which are potential homologues of yeast Ded1p and Dbp2p (34). We have, however, found the putative Ded1p homologue (Tb09.211.3510) in several other purifications, so the specificity of the interaction is unclear. PUF2 was pulled down, but subsequent co-IPs failed to show a specific interaction (not shown). The only other interaction of note was with a potential homologue of the yeast karyopherins Pse1p and Kap123p, encoded by Tb11.01.7010; this may have parallels in human cells since some components of the human NOT complex interact with the nuclear pore (9). Additional possible interaction partners included kinetoplastid-specific proteins of unknown function (see Supplementary Table S2).

Most NOT complex components are essential for the survival of *T. brucei*

To see whether *Tb*CNOT10 was essential in trypanosomes, we made permanent cell lines with tetracycline-inducible RNAi targeting *Tb*CNOT10 mRNA. Using the parasite form that lives in the mammal (bloodstream forms), we observed a severe proliferation defect within 36 h after RNAi induction (Figure 1C). In the slower growing procyclic form, a parasite stage that multiplies in Tsetse flies, it took ~60 h to observe a decrease in cell numbers. For comparison, we knocked down *TbNOT2* (Tb927.6.850), *TbNOT3/5* (Tb927.3.1920) and *TbCAF40* (Tb927.4.410) RNAs. Proliferation defects were seen for *TbNOT3/5* and *TbCAF40*, but not for *TbNOT2* (Supplementary Figure S2). In contrast, in the published high-throughput RNAi screen, *TbNOT2* RNAi also gave a growth defect (35). Our negative result for *TbNOT2* therefore could have been due to inadequate RNAi. The high-throughput screen (35) revealed growth defects for Tb927.8.1960 only during differentiation, and we too saw no defect after bloodstream-form RNAi (not shown).

Knowing that CNOT10 was essential, we could confirm the functionality of TAP-tagged CNOT10. In the line expressing the tagged version, we knocked out the remaining wild-type gene and found that the cells grew normally.

Depletion of *Tb*CNOT10 inhibits mRNA turnover and deadenylation

We next investigated the effect of *Tb*CNOT10 depletion on mRNA degradation, by inhibiting mRNA synthesis and processing, then measuring mRNA levels by northern blotting. Since all trypanosome mRNAs have the 39mer-spliced leader at the 5′-end, the turnover of bulk mRNA can be assessed by hybridization of northern blots with a spliced leader probe (36). Using this method with wild-type trypanosomes, half of the mRNA remained
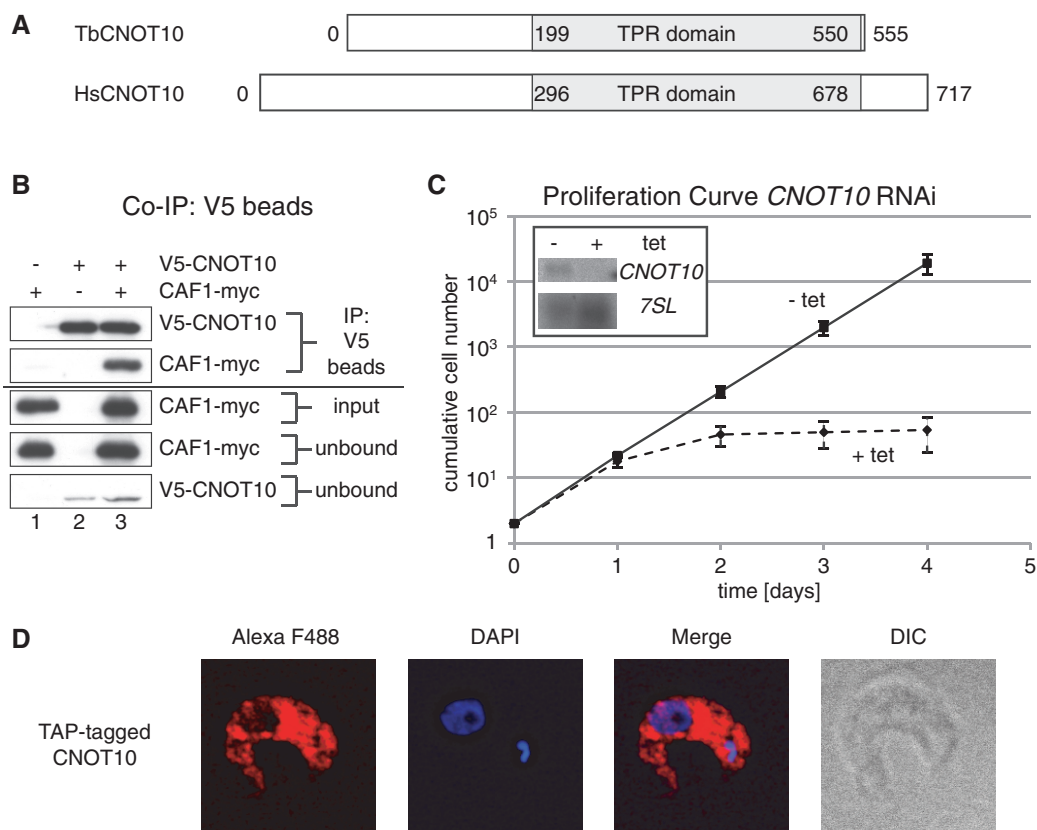
Figure 1. *Tb*CNOT10 is an essential and cytoplasmic protein in *T. brucei*. (**A**) Cartoon comparison of *T. brucei* and human CNOT10s. The conserved TPR domains are in grey. (**B**) Using anti-V5 beads, V5-*Tb*CNOT10 was pulled down from extracts of trypanosomes expressing *Tb*CAF1-myc (lane 1) V5-*Tb*CNOT10 (lane 2) or both tagged proteins (lane 3). A western blot was probed to detect the myc and V5 tags. The top two panels show the precipitated V5-*Tb*CNOT10 or *Tb*CAF1-myc from the three different cell lines. The next panel below is 1% of the input extract, and the two bottom panels are the unbound fractions. (**C**) Proliferation was measured in trypanosomes with tetracycline-inducible RNAi targeting *Tb*CNOT10 mRNA. Diamonds and dashed line represent *Tb*CNOT10 RNAi and black boxes and solid line represent uninduced cells. The northern blot (inset) shows the efficiency of RNAi after 24 h, with *7SL* RNA as control. (**D**) TAP-tagged *Tb*CNOT10 was detected by IF using rabbit polyclonal anti-protein A at 1:50 000. DAPI indicates the positions of the nucleus and kinetoplast (mitochondrial DNA). Differential interference contrast (DIC) microscopy shows the whole parasite.

after 30 min. After depletion of CNOT10, however, virtually no mRNA degradation was seen (Figure 2A). This indicated that *Tb*CNOT10 was important for overall mRNA degradation. Intriguingly, the spliced leader precursor (arrow) also appeared to have been stabilized.

Next, we studied three individual mRNAs, encoding actin (*ACT*), EP procyclin (*EP*) and histone H4 (*HISH4*). Degradation of each was inhibited (Figure 2B–D). In *Tb*CNOT10-depleted trypanosomes, both degradation of *ACT* mRNA was delayed. Moreover, the steady-state level of *ACT* increased ~6-fold after *Tb*CNOT10 depletion (Figure 2B). These effects were even more marked for *EP* mRNA, with the steady-state level increasing 3–4-fold (Figure 2C). We previously showed that *EP* mRNA degradation is biphasic, with an initial rapid degradation mediated by the 5′–3′ pathway, followed by a deadenylation-dependent phase which was inhibited by *CAF1* RNAi (37). Exactly the same was seen now for *CNOT10* RNAi (Figure 2C). The *HISH4* mRNA was also more stable after the RNAi, but there was no evident change in the steady-state level (Figure 2D, lanes 2 and 3). To visualize deadenylation, we ran a sample on a polyacrylamide gel,

flanked by marker lanes of fully deadenylated mRNA (treated with oligo d(T) and RNase H). Several polyadenylation sites are used (Figure 2D, lanes 1 and 10), and full-length polyadenylated mRNA forms a smear between 500 and 700 nt (lanes 2 and 3) (5). After transcription inhibition, the smear becomes progressively shorter (lanes 6 and 8), and this process was clearly delayed in cells with *CNOT10* RNAi (lanes 7 and 9). These results indicate that *Tb*CNOT10 is important for deadenylation and degradation of mRNAs in *T. brucei*.

*Tb*CNOT10 is important for association of *Tb*CAF1 with the NOT complex

To assess the effect of *Tb*CNOT10 depletion on the NOT complex, we analysed migration of different complex components by glycerol gradient centrifugation. For these experiments, we used equal mixtures of three cell lysates. Two lysates were always from cells expressing *in situ* V5-tagged versions of *Tb*NOT1 or *Tb*CNOT10. These were used to follow the position of the complex. Both *Tb*NOT1 and *Tb*CNOT10 migrated between fractions 9 and 20 (Figure 3A). The third lysate came from trypanosomes with *in situ* V5-tagged CAF1, with or without
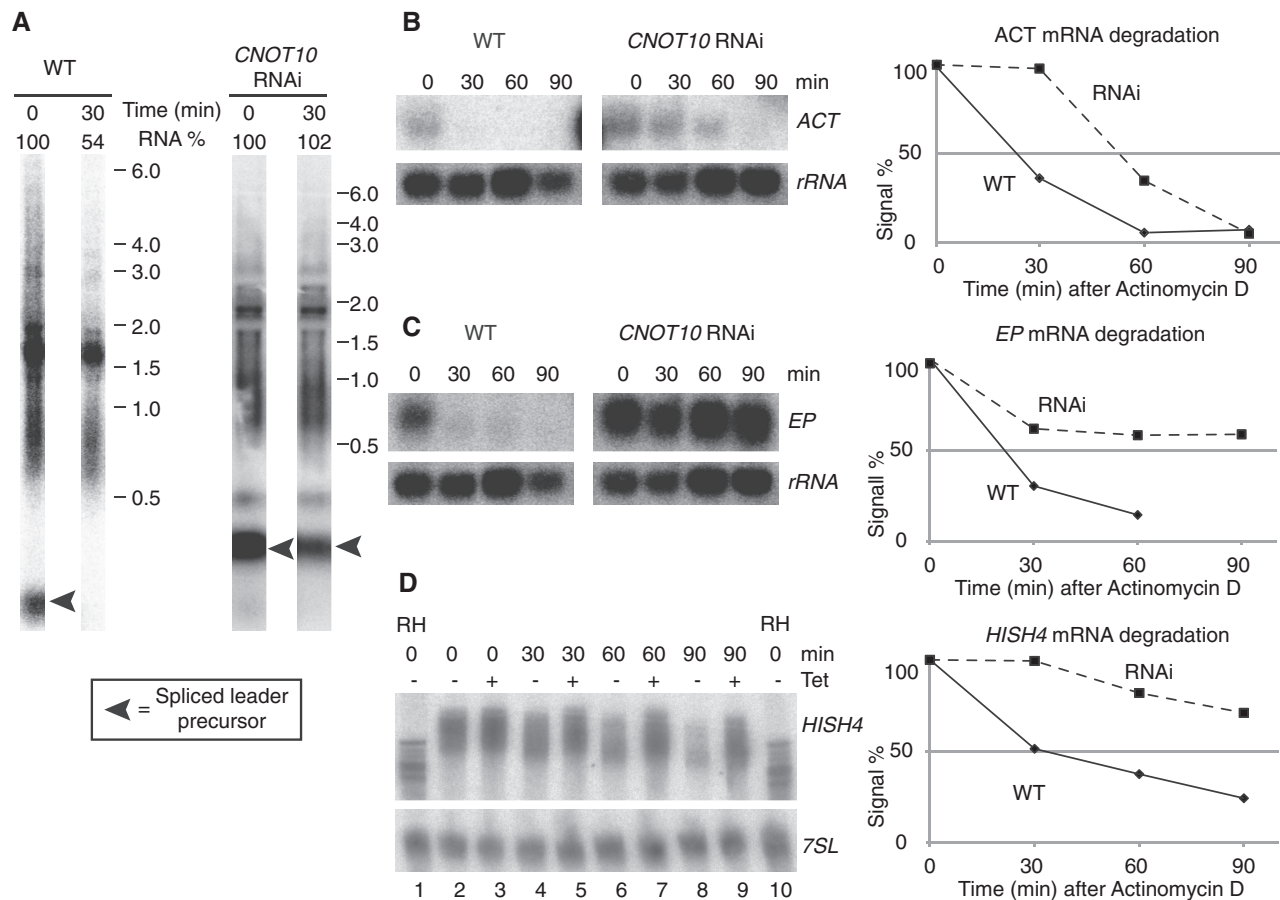
Figure 2. Effect of *Tb*CNOT10 depletion on mRNA degradation in trypanosomes. (**A**) Bulk mRNA turnover of wild-type cells and *Tb*CNOT10-depleted cells was analysed by hybridization of northern blots with a spliced leader probe. Transcription was inhibited and the signal was measured for two time points ($T = 0$ and 30 min). In each case, the signal of rRNA was used as a loading control. The northern blots from $T = 0$ and 30 min originate from the same gel, but were cut due to the loading of other samples in between. (**B–D**) *TbCNOT10* was depleted for 36 h by RNAi in *Tb*, then transcription was inhibited. RNA was prepared 0, 30, 60 and 90 min after the addition of actinomycin D. Wild-type cells were used as control. RNA levels were measured from northern blots probed for *ACT* (B), *EP* (C) and *HISH4* (D) mRNAs. In each case, the signal of rRNA was used as a loading control. The mean signal for *ACT* normalized to rRNA ($n = 6$) was plotted. The dashed line and square box represent RNAi and, diamonds and line represent wild type. The same was done for *HISH4* ($n = 4$) and for *EP* ($n = 6$). Sample agarose gels used for the half-life measurement are shown in (B) and (C). For *HISH4* (D, labelled as *H4*), we instead show a blot from a 4.5% denaturing polyacrylamide gel; mRNAs from cells with and without RNAi are alternately loaded in order to enable mRNA length comparisons. For lanes 1 and 10, RNA was treated with RNaseH and oligo d(T) in order to remove the poly(A) tails.

CNOT10 RNAi. In cells without RNAi, about half of the CAF1 was present in fractions 9–20 of the gradients, while the remainder was in lighter fractions (Figure 3A, C and D). We concluded that the NOT complex was concentrated in fractions 13–18, but that half of the CAF1 was not associated with it. In contrast, when we knocked down *TbCNOT10* by RNAi, *Tb*CAF1 no longer co-migrated with the complex at all (Figure 3B–D). This result suggested that *Tb*CNOT10 is essential for the interaction of *Tb*CAF1 with the rest of the NOT complex.

TbCNOT10 depletion reduces the level of TbNOT1

To define the interactions within the trypanosome NOT complex in more detail, we analysed them using the yeast two-hybrid system. The experiments showed that *Tb*CNOT10 interacted with *Tb*CAF1, *Tb*NOT5 and the N- and C-terminal parts of *Tb*NOT1 (Figure 4 and Supplementary Figure S3). The interaction between

*Tb*CNOT10 and *Tb*NOT5 was seen only with *Tb*CNOT10 as the prey and *Tb*NOT5 as the bait. *Tb*CAF1 interacted with *Tb*CNOT10 and the N-terminal part of *Tb*NOT1, but not with *Tb*NOT5. Interaction of *Tb*CAF1 with the C-terminal part of *Tb*NOT1 was only seen in one direction, under low stringency conditions (Supplementary Figure S3).

To find out whether *TbCNOT10* depletion directly affects the level of *Tb*CAF1 or *Tb*NOT1 in trypanosomes, we knocked down *TbCNOT10* in cells expressing *in situ*-tagged V5-*Tb*CAF1 or V5-*Tb*NOT1, and measured the proteins by western blot. The amount of V5-*Tb*CAF1 was not influenced by depletion of *Tb*CNOT10 (Figure 5A, lanes 3 and 4), but *Tb*NOT1 was decreased (Figure 5B, lanes 3 and 4).

The effect of *Tb*CNOT10 depletion on *Tb*CAF1 association was next investigated by co-IP. We first used trypanosomes with V5-tagged *Tb*NOT1 and inducible *Tb*CAF1-myc; note that the V5-NOT1 is likely to be at
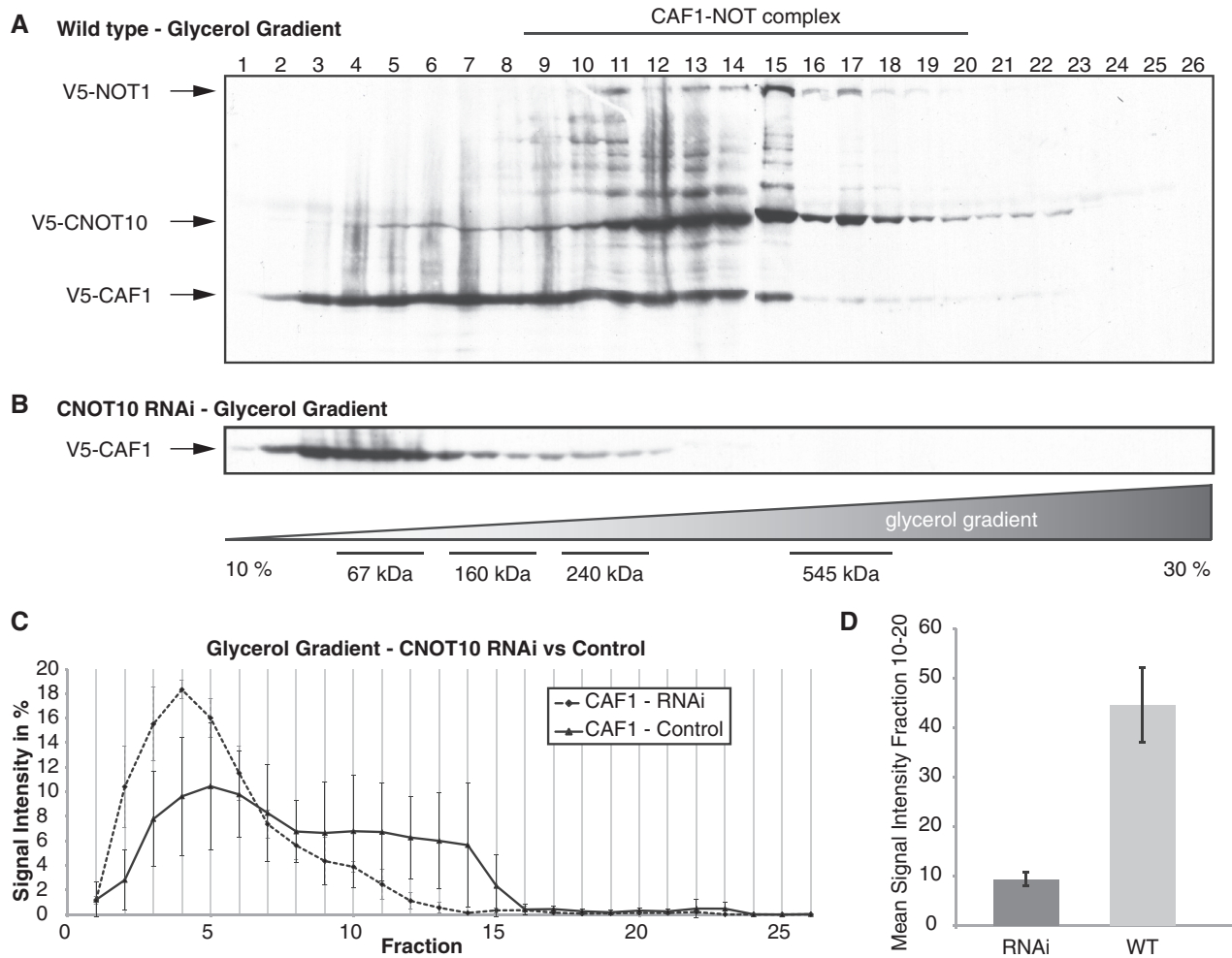
Figure 3. Depletion of *Tb*CNOT10 results in loss of *Tb*CAF1 from the trypanosome complex. (**A**) Extracts of three different trypanosome lines (*in situ* V5-tagged *Tb*CAF1, *Tb*CNOT10 and *Tb*NOT1) were mixed and run on a 10–30% glycerol gradient. The gradient was fractionated into 26 fractions. The additional bands between *Tb*NOT1 and *Tb*CNOT10 were degradation products of *Tb*NOT1. Size indications are shown in figure (**B**) at the bottom. (**B**) Glycerol gradient of *Tb*CNOT10-depleted cells with *in situ* V5-tagged *Tb*CAF1. (**C, D**) Quantification of the signals from three independent gradients. (**C**) For each fraction, the level of signal is expressed as the percentage of the total signal on the blot. V5-*Tb*CAF1 in *Tb*CNOT10-depleted cells (dashed line; *n* = 3) and control (black line; *n* = 3). A comparison of the V5-*Tb*CAF1 western blots signal from fractions 10–20 is shown in (**D**).
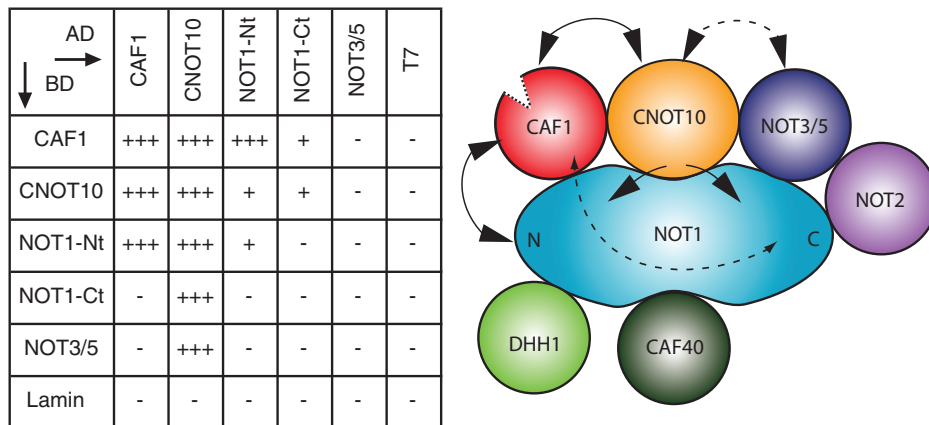
Figure 4. Yeast two-hybrid interactions in the trypanosome NOT complex. Left: minus and plus signs indicate the absence or presence of interaction detected by the activation of the *His3* and *LacZ* reporters; multiple pluses indicate the activation of the *Ade2*, *His3* and *LacZ* reporters. Lamin and T antigen (7) are negative controls. Right: illustration of the trypanosome NOT complex. Lines indicate interaction between different subunits, when the line is dashed, the interaction was shown only in one direction.
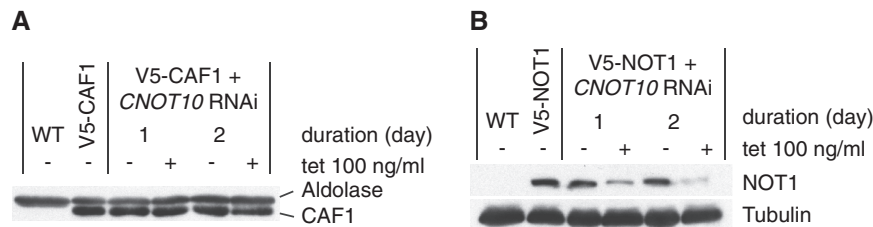
Figure 5. *TbCNOT10* knock-down leads to decrease of *Tb*NOT1 in trypanosomes. (**A**) The level of *in situ* V5-tagged *Tb*CAF1 was measured after *TbCNOT10* depletion. Extracts were made from wild-type cells (WT), cells with *in situ* V5-tagged *Tb*CAF1, and the same cells with inducible RNAi targeting *TbCNOT10*, with RNAi induced for either 1 or 2 days. The level of V5-*Tb*CAF1 was then measured by western blotting, with the aldolase signal as a control. (**B**) The effect of *TbCNOT10* RNAi on the level of *in situ* V5-tagged *Tb*NOT1 was analysed. The experiment is the same as in (A) except that in this case, the tagged protein was *Tb*NOT1 and tubulin was used as a control.

roughly endogenous levels whereas the CAF1-myc is over-expressed. Pull-down of *Tb*CAF1-myc yielded V5-*Tb*NOT1 as expected (Figure 6A, lane 6), though most of the V5-*Tb*NOT1 appeared not to be associated with *Tb*CAF1 (Figure 6A, lane 6). If all *Tb*NOT1 is associated with *Tb*CAF1, this could mean that there is much more untagged *Tb*CAF1 than *Tb*CAF1-myc in the cells; alternatively, perhaps some *Tb*NOT1 is not associated with *Tb*CAF1. When *TbCNOT10*-depleted trypanosomes were used, the amount of co-precipitated *Tb*NOT1 was reduced as expected (Figure 6A, lane 9). Thus, under the conditions used, *Tb*CNOT10 appeared to be limiting for the *Tb*CAF1–*Tb*NOT1 association. Using the same extracts, the reciprocal pull-down of V5-*Tb*NOT1 yielded *Tb*CAF1-myc as expected (Figure 6B, lane 6), although again most *Tb*CAF1-myc remained in the super-natant (Figure 6B, lane 8), consistently with the glycerol gradient result and the over-expression of *Tb*CAF1-myc. Puzzlingly, when *TbCNOT10*-depleted trypanosomes were used for the V5-*Tb*NOT1 pull-down, the amount of co-precipitated *Tb*CAF1-myc was only slightly affected even though the amount of precipitated V5-*Tb*NOT1 was lower (Figure 6B, compare lanes 6 and 9). This is difficult to explain because it is inconsistent with the other results; perhaps, it is connected with over-expression of *Tb*CAF1-myc.

Because of this result, we also used the association of *Tb*CAF40 to monitor complex integrity. In cells with normal amounts of *Tb*CNOT10, precipitation of *Tb*CAF1-myc resulted in co-precipitation of V5-*Tb*CAF40 (Figure 6C, lane 6), but this no longer occurred in *Tb*CNOT10-depleted trypanosomes (Figure 6A, lane 9). The results were confirmed by reciprocal pull down (Figure 6D, lanes 6 and 9).

Together, these results show that both *Tb*CAF1 and *Tb*CNOT10 interact directly with *Tb*NOT1, and that the presence of *Tb*CNOT10 enhances the interaction between *Tb*CAF1 and *Tb*NOT1. Depletion of *Tb*CNOT10, with the accompanying reduction in the *Tb*CAF1–*Tb*NOT1 interaction, reduces the cellular level of *Tb*NOT1.

CAF1 deadenylation activity is not complex dependent

One possible interpretation of all observations so far was that when *Tb*CAF1 is not in the NOT complex, it is unable to initiate mRNA degradation. However, we had previously shown that recombinant *Tb*CAF1 is active in

deadenylation *in vitro* (5). There are two possible explanations for this discrepancy. Either *Tb*CAF1 enzyme activity *in vivo* is dependent on, or stimulated by, inter-actions in the complex, or *Tb*CAF1 relies on the complex for attachment to substrates. To distinguish between these possibilities, we created a cell line containing a constitu-tively expressed mRNA reporter, which consisted of a *GFP* ORF followed by six boxB elements and an actin 3′-UTR (*GFP-B-ACT*). In addition, the cell line inducibly expressed a *Tb*CAF1 fusion protein with a λN peptide at the N-terminus and myc at the C-terminus (λN-*Tb*CAF1-myc). This hybrid protein should be 'tethered' to the *GFP-B-ACT* reporter RNA through the interaction between the B-boxes and the λN peptide. Upon induction of λN-*Tb*CAF1-myc expression, *GFP-B-ACT* mRNA was destroyed (Figure 7, lanes 1, 2 and 7, 8). A control RNA with no boxB (*GFP-ACT*) was unaffected by λN-CAF1-myc expression (not shown).

So far the tethering result did not tell us whether *Tb*CAF1 requires interaction with the NOT complex for its activity, since tethered λN-*Tb*CAF1-myc might still interact with the NOT complex. To reduce the interaction, we depleted *TbCNOT10* by RNAi. Now, λN-CAF1-myc alone should be tethered. Nevertheless, the *GFP-boxB* mRNA reporter was degraded as actively as before (Figure 7, lanes 3–6 and 9–12). This result suggests that *Tb*CAF1 does not depend on NOT complex association in order to degrade a tethered substrate. In other words, *Tb*CAF1 alone is indeed active *in vivo*, but it depends on the presence of *Tb*CNOT10—and, by extension, perhaps the rest of the NOT complex—to be recruited to its substrate.

HsCNOT10 is probably not required for association of HsCAF1 with the NOT complex

Knowing the importance of *Tb*CNOT10 in mRNA deg-radation, we were interested whether this function was conserved in mammalian cells. Therefore, we first con-firmed the interaction of *Hs*CAF1a and *Hs*CNOT10 in HEK 293 cells by co-IP (Figure 8A). Using myc-strep-tagged *Hs*CAF1a or *Hs*CAF1b, we were able to pull down endogenous *Hs*CNOT10 and could confirm the interaction previously shown by TAP (38). To determine whether the association of *Hs*CAF1a with core compo-nents of the human NOT complex is *Hs*CNOT10-dependent, we knocked down *Hs*CNOT10 by siRNA
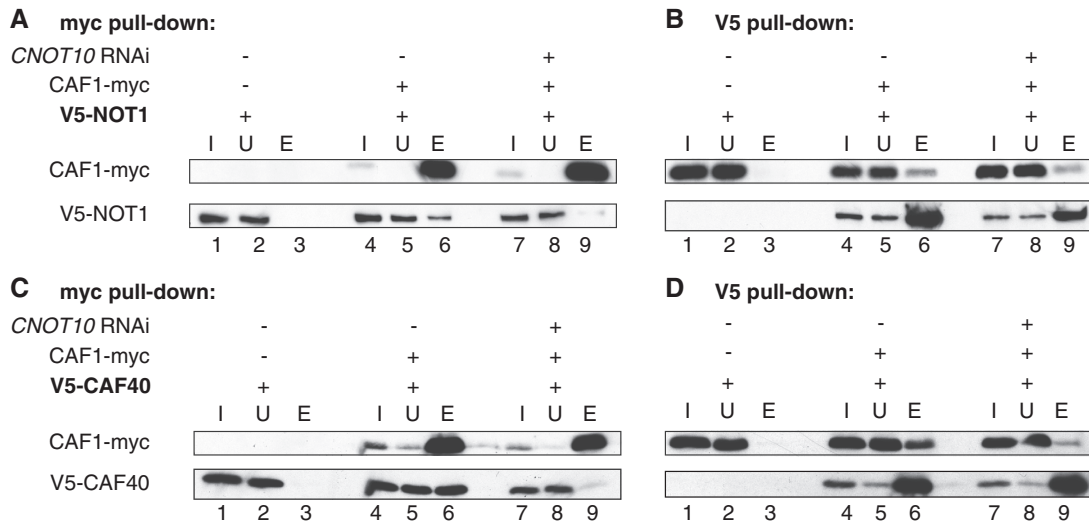
Figure 6. Depletion of trypanosome CNOT10 reduces CAF1 association with the complex. (**A**) myc-beads were used to pull down myc-tagged *Tb*CAF1 in normal trypanosomes (lanes 4–6) and cells with *TbCNOT10* RNAi (lanes 7–9). Trypanosomes, expressing V5-tagged *Tb*NOT1 without myc-tagged *Tb*CAF1, were used as a negative control (lanes 1–3). One percent was loaded for input (I) and unbound fraction (U) and the rest was eluted (eluate, E). (**B**) The reciprocal experiment using V5-beads. (**C, D**) as in (A, B), respectively, but here the interaction between *Tb*CAF1 and *Tb*CAF40 was analysed with or without *CNOT10* RNAi.
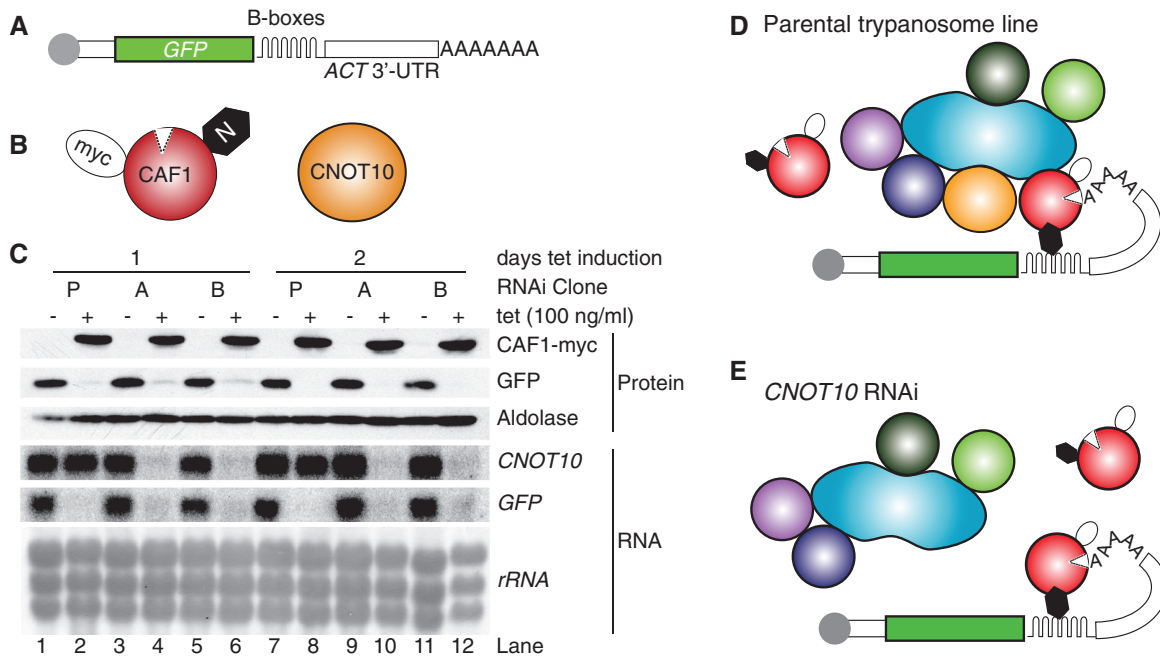
Figure 7. Tethered *Tb*CAF1 destroys a reporter mRNA in trypanosomes. (**A**) Cartoon of the reporter RNA, with a cap (grey) *GFP* ORF and six Bbox loops at the start of the 3′-UTR, (**B**) λN-*Tb*CAF1-myc is shown in red, and *Tb*CNOT10 is in orange. (**C**) Western (above) and northern blots showing expression of GFP protein and *GFP* mRNA, as well as *Tb*CAF1-myc, aldolase control and *TbCNOT10* RNA. Equal loading of the RNA was shown using rRNA. Results are shown for the parental cell line with no RNAi (P) and two independent clones with *CNOT10* RNAi, labelled A and B. (**D**) The situation in the parental cell line P—lanes 1, 2, 7 and 8 in (C). λN-*Tb*CAF1-myc is shown interacting with the B-boxes on the reporter and also with the rest of the NOT complex; the tethered CAF1 can degrade the poly(A) tail. (**E**) The situations in cell lines A and B, after induction of RNAi against *TbCNOT10* for 1 day (lanes 4 and 6 of (C)) or 2 days (lanes 10 and 12 of (C)). *Tb*CAF1 is still tethered to the reporter RNA and can still degrade poly(A), even though association with the NOT complex has decreased.

and analysed the migration of *Hs*CAF1a in a glycerol gradient. As controls we used a scrambled siRNA and a siRNA against *Hs*NOT1. Figure 8B shows that *Hs*CNOT10 depletion did not influence the migration of

*Hs*CAF1a, whereas knock-down of *Hs*NOT1 led to a shift of *Hs*CAF1a towards lighter fractions. The knock-down efficiency of *Hs*CNOT10 and *Hs*NOT1 was verified by western blot analysis (Figure 8C). We also attempted to

Figure 8. *Hs*CNOT10 is not required for association of CAF1 with the human NOT complex. (**A**) Myc-strep-tagged *Hs*CAF1a or *Hs*CAF1b were purified from HEK293 cells, and association of *Hs*CNOT10 was assessed by western blot analysis. Cells expressing the tag alone served as the control. (**B**) Control, human CNOT10 and NOT1 RNAi extracts were run on 10–30% glycerol gradients and 15 fractions were collected. Western blots of the gradient fractions were analysed for the migration of *Hs*CAF1a. The Ponceau-stained band is BSA, which was added to every fraction to serve as a control for equal precipitation efficiency. (**C**) *Hs*NOT1 and *Hs*CNOT10 depletion was confirmed by western blot analysis.

determine the effect of *Hs*CNOT10 depletion on Caf1b complex association, using a Caf1b-specific antibody. Results suggested that Caf1b also might have remained complex associated after *Hs*CNOT10 knock-down, but since Caf1b was extremely difficult to detect no firm conclusion could be drawn.

Notably, the knock-down of *Hs*CNOT1 reduced the amount of *Hs*CNOT10, whereas the reverse was not the case. These results suggested that *Hs*CNOT10 is not required for association of *Hs*CAF1a with *Hs*NOT1 in HEK293 cells.
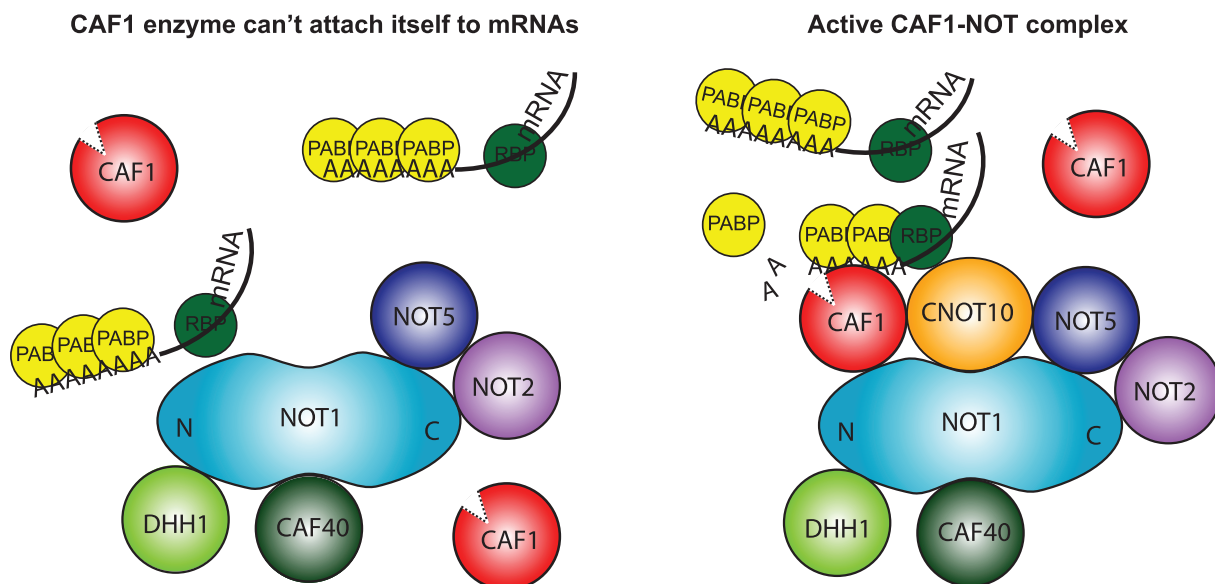
DISCUSSION

In this study, we have shown that in the relatively simple trypanosome NOT complex, association of *Tb*CAF1 with *Tb*NOT1 is enhanced by the presence of *Tb*CNOT10. Further, our results indicate that *in vivo*, this association is required for deadenylation of mRNAs by *Tb*CAF1.

Our yeast two-hybrid experiments revealed various interactions between *Tb*CNOT10, *Tb*CAF1, *Tb*NOT5 and the N- and C-terminal parts of *Tb*NOT1 (Figure 4). The two-hybrid interactions of *Tb*CAF1, *Tb*NOT5 and *Tb*CNOT10 with *Tb*NOT1 seem likely to be direct, as they parallel those seen in other species. The interaction between *Tb*CAF1 and *Tb*NOT1 most likely resembles that seen in opisthokonts (16,17). The relevant region of NOT1 is highly conserved across evolution and the most important CAF1-interacting residues of yeast and trypanosome NOT1s are identical. In CAF1, somewhat less conservation is evident in the interaction domain, but the overall hydrophobic character is conserved. In contrast, we cannot currently be sure that the apparent interaction between *Tb*CAF1 and *Tb*CNOT10 is direct, since we cannot rule out the possibility that they interact via

yeast Not1p. Given the sequence conservation, *Tb*CAF1 might indeed interact with yeast Not1p. In contrast, *Tb*CNOT10 bears no resemblance to any yeast protein (including Caf130p) so interaction with Not1p would not be expected.

TAP of CNOT10, bearing an N-terminal protein-A-calmodulin-binding-peptide tag, did not result in co-purification of *Tb*CAF1; exactly the same result was obtained for *Hs*CNOT10 bearing an N-terminal FLAG-HA tag (9). This was not caused by the buffer conditions since *Tb*CNOT10 was obtained after TAP of the complex using TAP-*Tb*CAF1. It was probably not caused by the tag either: N-terminally TAP-tagged *Tb*CNOT10 was functional, since trypanosomes expressing only the TAP-tagged version were viable, and *Tb*CNOT10 that was N-terminally fused with either the V5 peptide or yeast-two hybrid components, was able to interact with N- or C-terminally tagged *Tb*CAF1. The only explanation we can think of is that the interaction was somehow specifically competed by the binding of the tag to the resins.

In trypanosomes, *Tb*CNOT10 was required both for association of V5-*Tb*CAF1 with the complex, and for the presence of normal amounts of V5-*Tb*NOT1. The easiest explanation of this result is that *Tb*CNOT10, by interacting with both *Tb*CAF1 and *Tb*NOT1, stabilizes *Tb*CAF1–*Tb*NOT1 binding; and that *Tb*NOT1, which is not associated with *Tb*CAF1, is preferentially degraded.

Glycerol gradient analysis for both trypanosomes and HEK cells showed that about half of V5-*Tb*CAF1 or native *Hs*CAF1 was not associated with the NOT complex. The role of this 'free' fraction is not known. It may have no function at all, or it could have a role independent of deadenylation, for example in repressing translation, as shown for *Xenopus* oocytes (39). In addition, it could also act as a reserve stock for newly formed NOT

CAF1 enzyme can't attach itself to mRNAs

Active CAF1-NOT complex

Figure 9. A model for the function of *Tb*CNOT10 in trypanosomes. Left: in the absence of *Tb*CNOT10, *Tb*CAF1 is not able to bind PABP-covered mRNAs and initiate mRNA degradation. Right: upon association with the complex, *Tb*CAF1 is 'tethered' to target mRNAs through other subunits.

complexes. Since in trypanosomes, we saw a reduction in deadenylation and mRNA degradation in *Tb*CNOT10-depleted cells, with concomitant loss of CAF1 association with the NOT complex, it seems likely that *in vivo*, free *Tb*CAF1 is unable to digest PABP-coated poly(A) tails. In contrast, once *Tb*CAF1 attaches to an mRNA, either via the complex or by tethering, digestion is possible (Figure 9). Similarly, in human cells, depletion of *Hs*NOT1 or *Hs*NOT2 destabilized the NOT complex and decreased deadenylation (14,19), and the interaction of *Hs*CAF1a with *Hs*NOT1 was required for Caf1-/Not-dependent degradation of an miRNA target (16). In budding yeast, disruption of the interaction between the deadenylases (Ccr4p and Caf1p) and Not1p, effected by expression of dominant-negative interaction-defective mutants, impaired growth and deadenylation (17).

In human cells, the NOT complex can be recruited to mRNAs through RNA-binding proteins (e.g. (13)). We expect the same to be true in trypanosomes, but so far there are no good candidate RNA-binding proteins that might fill this role. In our TAP of the trypanosome NOT complex, we did not identify any RNA-binding proteins, but this is not surprising. Eukaryotic NOT complexes probably interact with many different proteins, so that any one would be present at relatively low levels. Moreover, such interactions may be transient. Indeed, human TTP, which does interact with human NOT complex, was not detected in pull-downs with any human NOT complex component (9).

We do not know which NOT complex subunits are directly responsible for interactions with RNA or RNA-binding proteins. Potential candidates for recruitment of the complex to human mRNAs are *Hs*CNOT3/5 and 9, both of which pulled down proteins with RNA-binding domains (9). In trypanosomes, recruitment of the NOT complex to different mRNAs through

different subunits could at least partially explain why all of the subunits are required for cell growth. The role of CNOT10 in human cells remains to be elucidated, but one possibility is that both human and trypanosome CNOT10 play roles in the targeting of mRNAs for degradation.

SUPPLEMENTARY DATA

Supplementary Data are available at NAR Online: Supplementary Tables 1 and 2 and Supplementary Figures 1–3.

REFERENCES

1. Chen,C.Y. and Shyu,A.B. (2011) Mechanisms of deadenylation-dependent decay. *Wiley Interdisc. Rev. RNA*, **2**, 167–183.

2. Wiederhold,K. and Passmore,L.A. (2010) Cytoplasmic deadenylation: regulation of mRNA fate. *Biochem. Soc. Trans.*, **38**, 1531–1536.

3. Tucker,M., Staples,R.R., Valencia-Sanchez,M.A., Muhlrad,D. and Parker,R. (2002) Ccr4p is the catalytic subunit of a Ccr4p/Pop2p/Notp mRNA deadenylase complex in *Saccharomyces cerevisiae*. *EMBO J.*, **21**, 1427–1436.

4. Temme,C., Zaessinger,S., Meyer,S., Simonelig,M. and Wahle,E. (2004) A complex containing the CCR4 and CAF1 proteins is involved in mRNA deadenylation in *Drosophila*. *EMBO J.*, **23**, 2862–2871.

5. Schwede,A., Ellis,L., Luther,J., Carrington,M., Stoecklin,G. and Clayton,C. (2008) A role for Caf1 in mRNA deadenylation and decay in trypanosomes and human cells. *Nucleic Acids Res.*, **36**, 3374–3388.

6. Collart,M. and Panasenko,O. (2012) The Ccr4-Not complex. *Gene*, **492**, 42–53.

7. Liu,H.Y., Badarinarayana,V., Audino,D.C., Rappsilber,J., Mann,M. and Denis,C.L. (1998) The NOT proteins are part of the CCR4 transcriptional complex and affect gene expression both positively and negatively. *EMBO J.*, **17**, 1096–1106.

8. Bai,Y., Salvadore,C., Chiang,Y.C., Collart,M.A., Liu,H.Y. and Denis,C.L. (1999) The CCR4 and CAF1 proteins of the CCR4-NOT complex are physically and functionally separated from NOT2, NOT4, and NOT5. *Mol. Cell Biol.*, **19**, 6642–6651.

9. Lau,N.C., Kolkman,A., van Schaik,F.M., Mulder,K.W., Pijnappel,W.W., Heck,A.J. and Timmers,H.T. (2009) Human Ccr4-Not complexes contain variable deadenylase subunits. *Biochem. J.*, **422**, 443–453.

10. Temme,C., Zhang,L., Kremmer,E., Ihling,C., Chartier,A., Sinz,A., Simonelig,M. and Wahle,E. (2010) Subunits of the *Drosophila* CCR4-NOT complex and their roles in mRNA deadenylation. *RNA*, **16**, 1356–1370.

11. Albert,T.K., Lemaire,M., van Berkum,N.L., Gentz,R., Collart,M.A. and Timmers,H.T. (2000) Isolation and characterization of human orthologs of yeast CCR4-NOT complex subunits. *Nucleic Acids Res.*, **28**, 809–817.

12. Fabian,M.R., Cieplak,M.K., Frank,F., Morita,M., Green,J., Srikumar,T., Nagar,B., Yamamoto,T., Raught,B., Duchaine,T.F. *et al.* (2011) miRNA-mediated deadenylation is orchestrated by GW182 through two conserved motifs that interact with CCR4-NOT. *Nat. Struct. Mol. Biol.*, **18**, 1211–1217.

13. Sandler,H., Kreth,J., Timmers,H.T. and Stoecklin,G. (2011) Not1 mediates recruitment of the deadenylase Caf1 to mRNAs targeted for degradation by tristetraprolin. *Nucleic Acids Res.*, **39**, 4373–4386.

14. Ito,K., Takahashi,A., Morita,M., Suzuki,T. and Yamamoto,T. (2011) The role of the CNOT1 subunit of the CCR4-NOT complex in mRNA deadenylation and cell viability. *Protein Cell*, **2**, 755–763.

15. Azzouz,N., Panasenko,O.O., Deluen,C., Hsieh,J., Theiler,G. and Collart,M.A. (2009) Specific roles for the Ccr4-Not complex subunits in expression of the genome. *RNA*, **15**, 377–383.

16. Petit,A.P., Wohlbold,L., Bawankar,P., Huntzinger,E., Schmidt,S., Izaurralde,E. and Weichenrieder,O. (2012) The structural basis for the interaction between the CAF1 nuclease and the NOT1 scaffold of the human CCR4-NOT deadenylase complex. *Nucleic Acids Res.*, September 12 (10.1093/nar/gks883; epub ahead of print).

17. Basquin,J., Roudko,V.V., Rode,M., Basquin,C., Seraphin,B. and Conti,E. (2012) Architecture of the nuclease module of the yeast Ccr4-Not complex: the Not1–Caf1–Ccr4 interaction. *Mol Cell.*, **48**, 207–218.

18. Russell,P., Benson,J.D. and Denis,C.L. (2002) Characterization of mutations in NOT2 indicates that it plays an important role in maintaining the integrity of the CCR4-NOT complex. *J. Mol. Biol.*, **322**, 27–39.

19. Ito,K., Inoue,T., Yokoyama,K., Morita,M., Suzuki,T. and Yamamoto,T. (2011) CNOT2 depletion disrupts and inhibits the CCR4-NOT deadenylase complex and induces apoptotic cell death. *Genes Cells*, **16**, 368–379.

20. Garces,R.G., Gillon,W. and Pai,E.F. (2007) Atomic model of human Rcd-1 reveals an armadillo-like-repeat protein with in vitro nucleic acid binding properties. *Protein Sci.*, **16**, 176–188.

21. Albert,T.K., Hanzawa,H., Legtenberg,Y.I., de Ruwe,M.J., van den Heuvel,F.A., Collart,M.A., Boelens,R. and Timmers,H.T. (2002) Identification of a ubiquitin-protein ligase subunit within the CCR4-NOT transcription repressor complex. *EMBO J.*, **21**, 355–364.

22. Dimitrova,L.N., Kuroha,K., Tatematsu,T. and Inada,T. (2009) Nascent peptide-dependent translation arrest leads to Not4p-mediated protein degradation by the proteasome. *J. Biol. Chem.*, **284**, 10343–10352.

23. Chen,J., Rappsilber,J., Chiang,Y.C., Russell,P., Mann,M. and Denis,C.L. (2001) Purification and characterization of the 1.0 MDa CCR4-NOT complex identifies two novel components of the complex. *J. Mol. Biol.*, **314**, 683–694.

24. Daniels,J., Gull,K. and Wickstead,B. (2010) Cell biology of the trypanosome genome. *Microbiol. Mol. Biol. Rev.*, **74**, 552–569.

25. Clayton,C. and Michaeli,S. (2011) 3′ processing in protists. *Wiley Interdiscip. Rev. RNA*, **2**, 247–255.

26. Michaeli,S. (2011) Trans-splicing in trypanosomes: machinery and its impact on the parasite transcriptome. *Future Microbiol.*, **6**, 459–474.

27. Manful,T., Fadda,A. and Clayton,C. (2011) The role of the 5′–3′ exoribonuclease XRNA in transcriptome-wide mRNA degradation. *RNA*, **17**, 2039–2047.

28. Clayton,C.E., Estevez,A.M., Hartmann,C., Alibu,V.P., Field,M. and Horn,D. (2005) Down-regulating gene expression by RNA interference in *Trypanosoma brucei*. *Methods Mol. Biol.*, **309**, 39–60.

29. Estevez,A.M., Kempf,T. and Clayton,C. (2001) The exosome of *Trypanosoma brucei*. *EMBO J.*, **20**, 3831–3839.

30. Clayton,C.E. (1987) Import of fructose bisphosphate aldolase into the glycosomes of *Trypanosoma brucei*. *J. Cell. Biol.*, **105**, 2649–2653.

31. Woods,A., Sherwin,T., Sasse,R., MacRae,T.H., Baines,A.J. and Gull,K. (1989) Definition of individual components within the cytoskeleton of *Trypanosoma brucei* by a library of monoclonal antibodies. *J. Cell Sci.*, **93(Pt 3)**, 491–500.

32. Altschul,S.F., Madden,T.L., Schaffer,A.A., Zhang,J., Zhang,Z., Miller,W. and Lipman,D.J. (1997) Gapped BLAST and PSI-BLAST: a new generation of protein database search programs. *Nucleic Acids Res.*, **25**, 3389–3402.

33. Gough,J., Karplus,K., Hughey,R. and Chothia,C. (2001) Assignment of homology to genome sequences using a library of hidden Markov models that represent all proteins of known structure. *J. Mol. Biol.*, **313**, 903–919.

34. Zinoviev,A., Akum,Y., Yahav,T. and Shapira,M. (2012) Gene duplication in trypanosomatids—two DED1 paralogs are functionally redundant and differentially expressed during the life cycle. *Mol. Biochem. Parasitol.*, **185**, 127–136.

35. Alsford,S., Turner,D.J., Obado,S.O., Sanchez-Flores,A., Glover,L., Berriman,M., Hertz-Fowler,C. and Horn,D. (2011) High-throughput phenotyping using parallel sequencing of RNA interference targets in the African trypanosome. *Genome Res.*, **21**, 915–924.

36. Kramer,S., Queiroz,R., Ellis,L., Webb,H., Hoheisel,J.D., Clayton,C. and Carrington,M. (2008) Heat shock causes a decrease in polysomes and the appearance of stress granules in trypanosomes independently of eIF2(alpha) phosphorylation at Thr169. *J. Cell Sci.*, **121**, 3002–3014.

37. Schwede,A., Manful,T., Jha,B., Helbig,C., Bercovich,N., Stewart,M. and Clayton,C. (2009) The role of deadenylation in the degradation of unstable mRNAs in trypanosomes. *Nucleic Acids Res.*, **37**, 5511–5528.

38. Gavin,A.C., Bosche,M., Krause,R., Grandi,P., Marzioch,M., Bauer,A., Schultz,J., Rick,J.M., Michon,A.M., Cruciat,C.M. *et al.* (2002) Functional organization of the yeast proteome by systematic analysis of protein complexes. *Nature*, **415**, 141–147.

39. Cooke,A., Prigge,A. and Wickens,M. (2010) Translational repression by deadenylases. *J. Biol. Chem.*, **285**, 28506–28513.